

# Frequency Analysis of the noise in the Fowler(n) sampling of a H2RG(2Kx2K) Near-IR Detector

G. Smadja<sup>1</sup>, C. Cerna<sup>2</sup>, A. Castera<sup>1</sup> and A. Ealet<sup>2</sup>

<sup>1</sup>IPNL, Institut de Physique Nuclaire de Lyon

4, rue Enrico Fermi, 69622, Villeurbanne cedex, France

<sup>2</sup>CPPM, Centre de Physique des Particules de Marseille

163 avenue de Luminy Case 902, 13288 marseille Cedex ,France

June 1, 2019

## Abstract

The readout noise of a H2RG HgCdTe NIR detector from Teledyne is measured at a temperature  $T=110\text{K}$ . It is shown that a Fowler mode with  $n = 240$  allows to reach a noise of  $2.63e$  (single read). A description of the power spectrum in terms of 3 parameters reproduces the variation of the noise as a function the number of Fowler samples, as well as its dependence on the periodicity of the sampling. The variance of the noise decreases with frequency with an effective power of 0.62 in our measurement domain. The behaviour of the detector under different experimental conditions can then be predicted.

## 1 The Apparatus

The measurements described in this paper were carried out in a dedicated setup built to evaluate Hawaii 2RG (HgCdTe) detectors from Teledyne. The detector was on loan from LBNL in view of the evaluation of its performance

when used in a spectrograph for the JDEM project [1]. The cryostat can be operated in a range of temperature extending from 110K to 160K with fluctuations smaller than 0.1 K, and its equilibrium temperature in the absence of heating is about 110K. The polarisation of the substrate was chosen as  $V_{sub} - V_{reset} = 0.4$  V in all the data analysed in this work. Additional experimental details are provided in a previous paper [2] where the conversion factor of our setup (e/ADCU) at  $T = 110$ K was evaluated to be 2.042 e/ADU for a single pixel. The goal of the present measurements is to lay the ground for a determination of the frequency distribution of the noise, so as to be able to predict the behaviour of the detector in different experimental conditions (Fowler samplings, interval between groups, etc...). The merit of the power spectrum analysis is also the link it provides with the physical processes in the CMOS semi-conductor, such as the trapping and detrapping of electrons with a distribution of time constants.

## 2 The measurement method

In the 2Kx2K H2RG detector, a window of 31x31 pixels has been selected. The clock frequency is 100kHz, as anticipated in the SNAP-JDEM project, and the time needed for the readout of 1 frame of 30x30 pixels is  $\delta = 17.5$ ms . The non destructive frame readouts are organised into 'groups' of 250 frames, read at the clock frequency of 100kHz and separated by a time interval which can be tuned, with the clocking of the pixels stopped. Taking into account the readout of the frames, the periodicity of the readout of a given pixel between 2 consecutive groups varies from 5s to 13s. The selection of a small window allows to reach a higher repetition rate for the frame readout, and to save on the overall measurement time as well as on computing resources. All the frames are stored on disk for further analysis. The noise is characterised by two variance measurements:

-the frame to frame variance, with the readout interval of  $\delta = 17.5$ ms for a 'window' frame 31x31 as considered here, is convenient for a calibration of the detector and its readout. It was studied in [2].

-the Fowler( $n$ ) group to group variance measured by the spread of the difference of the averages of 2 consecutive groups for a given pixel will allow to characterize the noise performance of the H2RG on longer time scales, and will be investigated here.

The Fowler( $n$ ) noise is evaluated in each pixel from the differences  $D_k$  of the average signal in groups  $k$  and  $k - 1$ .

$$D_k = \frac{1}{n} \sum_{i=1}^{i=n} s_{(t_0+k\Delta+i\delta)} - s_{(t_0+(k-1)\Delta+i\delta)} \quad (1)$$

The number of frames is 250 in the acquisition, but will be varied from 1 to 240 in the offline analysis as the first 10 frames of each group are always ignored. The noise is measured by the average of  $D_n(\Delta)^2$  over the  $N + 1$  groups stored during the exposure. The number of groups in the on-line acquisition was actually 200 in the exposures studied here, but the first 10 groups were eliminated from our investigation.

$$\sigma^2 = \frac{1}{N-1} \left( \sum_{k=1}^N (D_k - \langle D_k \rangle) \right)^2 \quad (2)$$

with

$$\langle D_k \rangle = \frac{1}{N} \left( \sum_{k=1}^N D_k \right) \quad (3)$$

The subtraction of the reference channel, which follows synchronously the level of a fixed capacitance, and corrects possible bias changes reduces the variance when the number of Fowler samplings  $n < 10$ , as shown in Figure 1 for a group periodicity of 5.23s. For larger numbers of reads, the variance of the noise is however slightly increased, by typically  $0.1\text{ADU}^2$ . We attribute this to low frequency voltage offsets, which are at least partially cured by the next step.

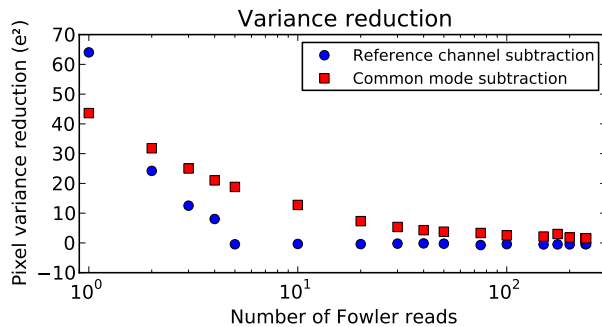


Figure 1: Noise reduction from reference channel and common mode subtractions. The second one is applied on top of the first one

### 3 Common-mode subtraction at low frequency

The reference channel subtraction takes out most of the high frequency common modes, but we still observe the impact of common modes remaining at lower frequencies in Figure 2a). This figure shows the remaining correlation between the differential flux observed for 2 randomly selected pixels between 2 consecutive groups (in the absence of any illumination), and the differential flux of the sum over all pixels. Both are averaged over the 240 Fowler acquisitions of the group, and the 200 groups of the exposure are shown. The value of the slope of the correlation is stored for each pixel, and its distribution is shown for all pixels in Figure 2b), where it is seen to

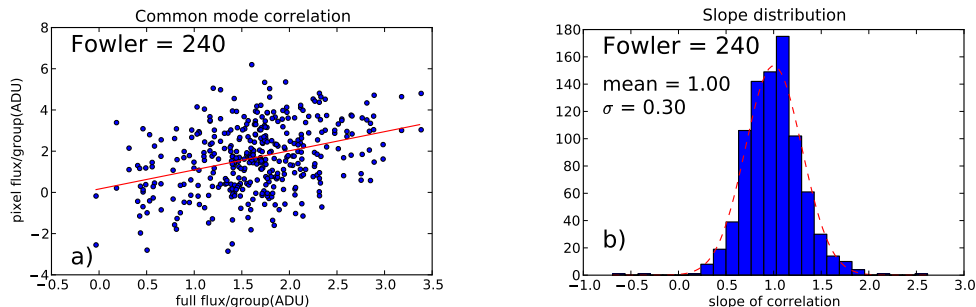


Figure 2: a) group to group correlation between pixel flux (Fowler=240) and full flux: 2 pixels have been selected at random. b) distribution of the correlation slope (Fowler = 240) found for all pixels

be compatible with unity within the measurement errors from the noise. A 'common' offset for each group is then obtained from a second straight line fit throughout the 'full' (integrated over all pixels) observed fluxes of all 200 groups as a function of the group number. The resulting variance reduction is shown in Figure 1 as a function of the Fowler number  $n$ , and the resulting distribution of the 240 corrected flux differences  $D_k$  is shown in fig 3, for a typical exposure at 110K with Fowler samplings  $n = 240$ . The rms of the distribution is 4 electrons. As this value arises from the difference between the averages over 2 (consecutive) groups of 240 frames, it can then be considered that the noise in a single Fowler readout is 2.85 electrons. We shall see in section 5 that part of this noise can be assigned to a parasitic photon flux, and that the actual performance reached is better. The improvement

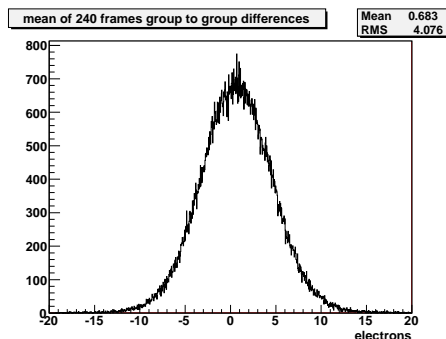


Figure 3: group to group difference distribution for Fowler(240)

observed with this common-mode subtraction may be a combination of intrinsic detector readout properties and of the specific implementation of the outside low voltage supplies.

## 4 Evolution with the number of samplings

The evolution of the variance of the difference  $D_k$  between consecutive groups as a function of the Fowler( $n$ ) number is shown in Figure 4 for an intergroup periodicity of 5.23s after the reference channel and common mode corrections have been applied. The duration of the full exposure (250 groups of 250 frames each) is 1280 seconds. The value reached for Fowler(240) corresponds to a noise of 2.85e for a single group read. It is apparent that the variance does *NOT* decrease like  $1/n$ , as would be expected for independent measurements, which would lead to a group to group noise of 1.6e at  $n = 240$ . There are two main contributions to these correlations: the non destructive readout itself, and the time domain correlations induced by the trapping and detrapping of electrons. This behaviour has been noted in several previous publications, such as [3], [4], [5], and implies the presence of time dependent correlations, which can be described by a frequency power spectrum. The connection between the time constant of trapping sites and the frequency power spectrum was first stated by [7], and a recent presentation can be found in the lectures of [8].

## 5 The extra flux

Before turning to the frequency power spectrum, we must take care of the other contributions to the observed variance. Even in the absence of any illumination inside the cryostat, The ADC level rises linearly with time, at the rate of 0.6 e/pix/s whatever the group periodicity. This rate is not a leakage current, as it is (almost) insensitive to the operating temperature, but it could be due either to a parasitic photon source or to some baseline drift. We shall assume here that the cause is a photon source subject to stochastic fluctuations, and we consider that the quantitative agreement with the data reached under this assumption argues in its favour. The impact of such a constant photon source on the Fowler( $n$ ) variance is recalled in Appendix A for completeness, although it has already been evaluated in the literature in a slightly different context, such as in [6], where the impact on a straight line fit is directly evaluated. The result is of the form

$$\langle P_n^2 \rangle = DI + f di_f \quad (4)$$

where  $\langle P_n^2 \rangle$  is the flux contribution to the variance,  $DI$  the intergroup contribution (the flux already included in the  $n$  Fowler frames must be omitted),  $di_f$  the frame to frame contribution, and the factor  $f$  takes into account the correlations arising from the non destructive readouts, as shown in Appendix A.

$$f = \frac{2di_f}{n^2} \cdot \frac{n(n-1)(2n-1)}{6} \quad (5)$$

## 6 Frequency spectrum of the noise

We show in Appendix B how to relate the Fowler averaging to the auto-correlation products. As the autocorrelation of the noise is itself directly related to the frequency power spectrum  $f(\omega)$ , the group to group noise for any number of Fowler samplings can then be expressed in terms of the power spectrum:

$$\langle s_t s_{t+\tau} \rangle = \int_{\omega_1}^{\omega_2} d\omega \cos(\omega\tau) f(\omega) \quad (6)$$

The power spectrum  $f(\omega)$  will be assumed to be of the form

$$f(\omega) = A + \frac{B}{\omega^\alpha} \quad (7)$$

If this functional dependance were exact, the white 'thermal' amplitude  $A$  would be a positive number, and  $\alpha$  might generally be expected to be close to 1. Our measurements are however performed in a frequency range where the white noise is subdominant, so that  $A$  is just a parameter of the fit, and it turns out it will be found to be small and negative. The power  $\alpha$  found is also an effective power in our frequency range, which may combine the detector and FET effects. The merit of this 3 parameter formalism is that it describes the shape of the Fowler ( $n$ ) function with an accuracy of 2% and has a predictive power for different group or frame periodicities as well.

As shown in Appendix B, the measured variance  $\langle D_n(\Delta)^2 \rangle$  can be expressed as a sum of autocorrelation products, and an explicit expression of the integral relating the power spectrum  $f(\omega)$  to the measured variance  $\langle D_n(\Delta)^2 \rangle$  is derived in the appendix:

$$\begin{aligned} \langle D_n^2 \rangle &= \int d\omega (1 - \cos\omega\Delta) \left( A + \frac{B}{\omega} \right) \\ &\cdot \left[ \frac{2}{n} + \frac{\mathcal{M}}{n \sin(\omega\delta/2)} + \frac{\mathcal{N}}{n^2 \sin^2(\omega\delta/2)} \right] \end{aligned} \quad (8)$$

With :

$$\mathcal{M} = 4 \cos\left(\frac{n\omega\delta}{2}\right) \sin\left(\frac{(n-1)\omega\delta}{2}\right)$$

and

$$\mathcal{N} = 1 - \cos(n\omega\delta) - 2n \sin\left(\frac{\omega(2n-1)\delta}{2}\right) \sin\left(\frac{\omega\delta}{2}\right)$$

In this relation,  $\delta$  and  $\Delta$  are the frame to frame and group to group periodicities. The predicted variance for given values of  $A, B$ , and the power

$\alpha$ , are evaluated at 10 different Fowler samplings (to spare computer time) and they are adjusted to the data for 2 different group periodicities of 5.23s and 13.11s by minimizing the  $\chi^2$ . Given the very high statistical accuracy of the measurements, and their reproducibility, the typical computed errors on each data point in Figure 4 is 3 to 4  $10^{-3}$ . On the other hand, the 3 parameter model used for the power spectrum reproduces the data to an accuracy of 1 to 2% for the best fits. The errors were rescaled to match this difference and follow the observed trend, as seen in Table 1.

The best fits differ for the 2 data samples, although the power spectra found are close to each other. The estimated increase in the noise at Fowler=240 is shared equally (in terms of variance) between the stochastic contribution and the 1/f contributions.

The (dominant) B contribution amounts to  $27.107e/(\text{Hz})^{-1/2}$  (5s intergroup) and  $29.096e/(\text{Hz})^{-1/2}$  (13s intergroup). The result of the fit is seen in Figure 4a, and the estimated errors on  $A$  and  $B$  shown as contour plots in Fig 4b) are only indicative, as the errors are just set so that the  $\chi^2/Ndf$  would be of the order of unity.

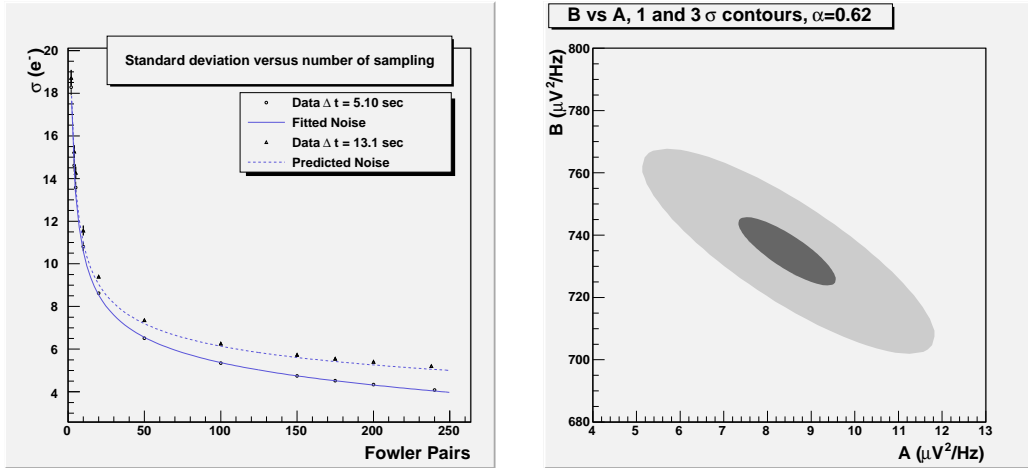


Figure 4: a) Fowler (n) noise measurement and adjusted frequency spectrum at a group periodicity of 5.23s b) contour plot of the A and B errors

## 7 Prediction of the group periodicity dependence

We can also check how accurately the evolution with the group period is predicted from the restricted lever arm in frequency provided by the Fowler(n) dependence of the noise at a single delay. We show in table 3 the dependence of the variance expected with 240 Fowler samples on the intergroup

Table 1: *Variance evolution with the number of Fowler samplings)*

Intergroup periodicity 5.23s, exposure time = 1280s				
Fowler nb.	Adjusted noise	Meas. noise	Meas. error	Assigned error
(n)	(e)	(e)	(e)	(e)
2	18.58	18.28	0.135	0.37
4	14.37	14.61	0.055	0.29
5	13.29	13.58	0.033	0.27
10	10.57	10.81	0.022	0.22
20	8.55	8.62	0.025	0.086
50	6.56	6.51	0.045	0.065
100	5.37	5.34	0.050	0.053
150	4.75	4.74	0.040	0.047
175	4.52	4.52	0.030	0.045
200	4.32	4.34	0.023	0.043
240	4.04	4.08	0.017	0.041
intergroup periodicity 13.11s, exposure time = 3275s				
Fowler nb.	Adjusted noise	Meas. noise	Meas. error	Assigned error
(n)	(e)	(e)	(e)	(e)
2	19.04	18.72	0.025	0.37
4	15.02	15.26	0.032	0.30
5	13.98	14.27	0.050	0.28
10	11.35	11.56	0.064	0.23
20	9.40	9.40	0.040	0.094
50	7.43	7.35	0.037	0.073
100	6.30	6.26	0.032	0.063
150	5.74	5.73	0.031	0.057
175	5.54	5.55	0.030	0.055
200	5.37	5.40	0.032	0.054
240	5.15	5.20	0.031	0.052

delay. The stochastic Poisson contribution from the assumed 'extra flux' is substantial, and the agreement with the observations suggests that the general features of the physical contributions to the noise are understood. A small discrepancy is observed at a group periodicity of 13s, confirmed by an inspection of the full Fowler prediction in Figure 4a). We are tempted to assign this effect to a frequency dependence of the power  $\alpha$ , which will be

Table 2: Adjusted power spectrum parameters at 5.23 and 13.11s group periodicities

Exposure time/ period(s/s)	Thermal A ( $\mu\text{V}^2\text{Hz}^{-1}$ )	1/f B ( $\mu\text{V}^2\text{Hz}^{-1}$ )	1/f power $\alpha$	$\chi^2/\text{Ndf}$
1280/5.23	8.445	734.819	0.62	6.063/8
3280/13.11	-1.525	846.563	0.57	6.000/8

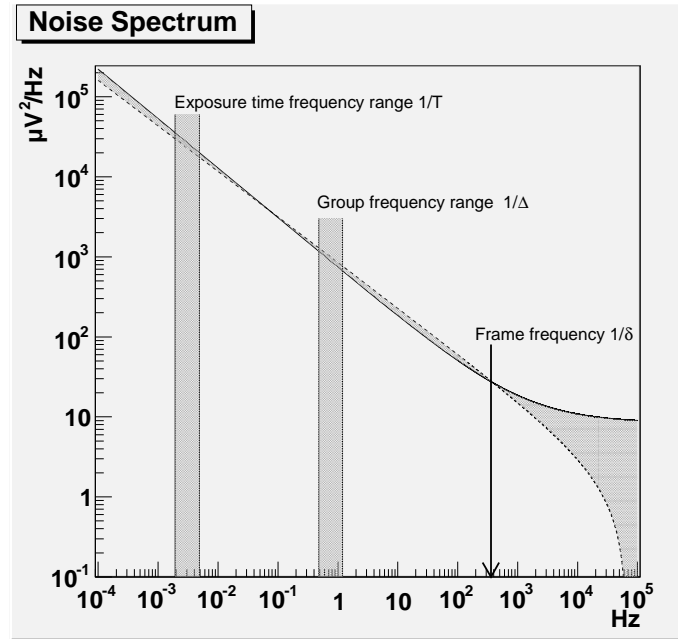


Figure 5: Frequency power spectrum of the noise with the adjusted parameters at group periodicities of 5.23 (continuous line) and 13.11s (dashed)

investigated in a later work.

Table 3: Variance evolution with group periodicity for Fowler(240)

Period/Exp. time (s)/(s)	Var. ( $e^2$ ) (flux)	Var. ( $e^2$ ) (frequency)	Var. ( $e^2$ ) (predicted)	Var. ( $e^2$ ) measured
5.23/1280	2.396	13.764	16.160	16.646
6.578/1315	3.427	14.949	18.376	18.768
7.304/1461	3.941	15.452	19.393	19.564
8.756/1751	4.905	16.085	20.991	21.328
10.208/2042	5.956	16.667	22.623	23.088
13.112/3275	8.066	17.472	25.538	27.041

It is seen that the actual readout contribution to the group to group variance is  $13.8 e^2$ , i.e. 3.71 electron for the difference between 2 Fowler(240) readouts and a group periodicity of 5.23s . The extrapolation of the parameters adjusted at an intergroup period of 5.23s is compared to the full Fowler(n) curve at a period of 13.11s in Figure 4a. It is seen that the predicted noise slightly underestimates the measured one, as also observed in table 3. The adjustment at a period of 13.11s has an unphysical negative value of the white noise component, as seen in Table 2 and Figure 5a). This feature has a minor impact as all the experimental data is carried in a frequency range smaller than 370 Hz, where the 2 frequency spectra are close to each other.

## 8 Conclusion

We have shown that the combined use of the reference channel and a common-mode correction lead to a significant reduction of the detector noise. The second correction can be performed with the help of non illuminated pixels (unavailable in the window mode) in the standard operation of the H2RG detector. With the H2RG lot # 40 which we measured, we reach a noise of 2.63e (single read) with Fowler(240) in a 1250s exposure. This is degraded to a noise of 2.96 e for a 3280s exposure with an intergroup periodicity of 13s. A description of the power spectrum of the noise in terms of 3 parameters also accounts quantitatively for the Fowler(n) variation of the noise at different group periodicities within an accuracy of 2%. The power law exponent found to reproduce the data is about 0.62. This 'effective' power law is only approximate, and the impact of additional parameters improving the description of the power spectrum will be investigated in a later work, as well as the effect of different polarisation voltages.

## 9 Acknowledgements

We thank all the institutions who have supported us during this work: Université Claude Bernard Lyon 1, The IN2P3/CNRS institute, and the engineers and technicians at IPNL and CPPM who have contributed to the apparatus F. Charlieux, J. C. Ianigro, P. Karst, and in particular C. Girerd who has designed the readout electronics. We are indebted to C. Bebek (LBNL) for lending us the H2RG detector, and to G. Tarle, M. Schubnell, and R. Smith for many questions and suggestions.

## References

- [1] M.-H. Aumeunier et al., Proc. SPIE 6265 (2006) 626534
- [2] G. Smadja et al., Measurement of the non-linearity and interpixel capacitance of a H2RG(2Kx2K) near IR detector Nuclear Instruments and Methods in physics Research A 610(2009)615
- [3] G. Finger et al. Performance of large format 2Kx2K MBE grown HgCdTe Hawaii-2RG arrays for low flux applications, Proceedings SPIE The International Society for Optical Engineering 2004, Vol. 5499, p.47
- [4] R. Smith and al. Noise and zero point drift in 1.7  $\mu\text{m}$  cutoff detectors for SNAP High Energy, Optical, and Infrared Detectors for Astronomy II, SPIE Vol. 6276, pp.62760R (2006)
- [5] M. Schubnell et al. Near Infrared Detectors for SNAP High Energy, Optical, and Infrared Detectors for Astronomy II, SPIE Vol. 6276, 62760Q, (2006).0277-786X/06/\$15  
Noise and Zero point drift in 1.7  $\mu\text{m}$  cutoff detectors for SNAP
- [6] B. J. Rauscher et al. Detectors for the James Webb Space Telescope Near-Infrared Spectrograph: Readout mode, Noise Model, and Calibration Publications of the Astronomical Society of the Pacific, 2007, Vol. 119, nb 857, p. 768
- [7] W. Schottky, Small-shot effect and Flicker effect, Phys. Rev. 28 (1926) 74
- [8] Y. Yamamoto, 1/f noise and random telegraph Signals. <http://www.stanford.edu/~rsasaki/EEAP248/chapter9.pdf>

# Appendix

## A Flux and leakage current contribution

$\delta$  and  $\Delta$  will be the interval between frames and between groups. In the Fowler mode, an average is taken between signals at  $t, t + \delta, t + 2\delta, \dots, t + (n - 1)\delta$  and the difference is formed with the homologous signal values at  $t + \Delta, t + \Delta + \delta, t + \Delta + 2\delta, \dots, t\Delta + (n - 1)\delta$ . The contribution of the stochastic fluctuation is evaluated next  $DI$  and  $di$  will be the mean intergroup and frame to frame fluxes,  $\delta(DI)$  will stand for the intergroup signal fluctuation, and  $\delta_i(k)$  will be the flux fluctuation of group  $i$  at frame  $k$  (the fluctuation of the difference between frames  $k$  and  $k - 1$ ).

$$\begin{aligned}
 S_1 &= DI + \delta(DI) \\
 S_2 &= DI + \delta(DI) + di + \delta_2(2) - \delta_1(2) \\
 S_3 &= DI + \delta(DI) + 2di + \delta_2(2) + \delta_2(3) - \delta_1(2) - \delta_1(3) \\
 S_4 &= DI + \delta(DI) + 3di + \delta_2(2) + \delta_2(3) + \delta_2(4) - \delta_1(2) - \delta_1(3) - \delta_1(4) \\
 S_n &= DI + \delta(DI) + (n - 1)di + \delta_2(2) + \dots + \delta_2(n) - \delta_1(2) - \dots - \delta_1(n)
 \end{aligned}$$

The average is formed

$$S = \frac{S_1 + S_2 + S_3 + \dots + S_n}{n}$$

The fluctuating Poisson contribution to the result is

$$\frac{1}{n}(\delta_2(2) - \delta_1(2)) * (n - 1) + (\delta_2(3) - \delta_1(3)) * (n - 2) + (\delta_2(4) - \delta_1(4)) * (n - 3) + \dots + (\delta_2(n) - \delta_1(n)) * 1$$

The variance of  $\delta_2(i)$  and  $\delta_1(i)$  are all equal to the number of electrons between 2 frames  $di_f$  (in number of electrons)

$$\delta(S)^2 = DI + \frac{1}{n^2} 2di_f^2 (1 + 2^2 + 3^2 + \dots + (n - 1)^2)$$

where the sum of the  $n - 1$  first squares appears

$$1^2 + 2^2 + 3^2 + \dots + (n - 1)^2 = \frac{(n - 1)(n)(2n - 1)}{6}$$

The stochastic contribution to the variance Fowler(n) variance will be (in electron units)

$$\delta(S)^2 = DI + \frac{1}{n^2} 2di_f^2 \frac{(n - 1)(n)(2n - 1)}{6} \quad (9)$$

To be added quadratically to the frequency spectrum noise. It is seen that the stochastic error on the group average grows like the number of Fowler averages, and will exceed the readout error at some point. High Fowler numbers harm at large fluxes.

## B The Wiener relation

Time domain correlations of the noise are induced by the interplay of the physical properties of semi-conductors. As shown by Wiener, they can be described by the frequency power spectrum of the noise, which happens to have a quasi universal behaviour as a function of frequency, of the form  $A + B/\omega^\alpha$ . Assume

$$x(t) = \int d\omega f(\omega) e^{-i\omega t}$$

$$\begin{aligned} \langle x(t)x(t + \Delta) \rangle &= \lim_{T \rightarrow \infty} \frac{1}{2T} \int_{-T}^{+T} dt d\omega_1 d\omega_2 e^{-i\omega_1 t} e^{i\omega_2 t + \Delta} f(\omega_1) f^*(\omega_2) \\ &= \lim_{T \rightarrow \infty} \frac{2\pi}{2T} \int d\omega e^{i\omega \Delta} f(\omega) f^*(\omega) \end{aligned}$$

As the result should be real

$$f(-\omega) = f(\omega)^*$$

$$\langle x(t)x(t + \Delta) \rangle = \frac{\pi}{T} \left( \int_0^\infty d\omega f(\omega) f(\omega)^* e^{i\omega \Delta} + \int_{-\infty}^0 d\omega f(\omega) f(\omega)^* e^{i\omega \Delta} \right)$$

So that taking advantage of the reality relation

$$\begin{aligned} \langle x(t)x(t + \Delta) \rangle &= \frac{\pi}{T} \int_0^\infty d\omega (e^{i\omega \Delta} + e^{-i\omega \Delta}) f(\omega) f(\omega)^* \\ &= \frac{2\pi}{T} \int_0^\infty d\omega \cos(\omega \Delta) f(\omega) f(\omega)^* \end{aligned}$$

including the factor  $2\pi/T$  in the normalisation of the power spectrum  $f$

$$\langle x(t)x(t + \Delta) \rangle = \int_0^\infty d\omega \cos(\omega \Delta) f(\omega) f(\omega)^* \quad (10)$$

The shape of the power spectrum  $|f(\omega)|^2$  will be assumed to be of the form

$$|f(\omega)|^2 = A + \frac{B}{\omega^\alpha}$$

where  $A$  is the intensity of the white noise component and  $B$  related to the strength of the  $1/\omega$  ( $1/f$ ) contributions.

## C The group to group averages

The measured quantity is the variance group to group differences in the Fowler(n) averages. We introduce the time intervals  $\delta$  between 2 reads of the same pixel in consecutive frames, and the equivalent interval  $\Delta$  between two readouts of the same pixel in the same frame in consecutive groups.

For the consecutive groups  $k$  and  $k + 1$

$$D_k = \frac{1}{n}(x(t_k+\Delta)-x(t_k)+x(t_k+\delta+\Delta)-x(t_k+\delta)+x(t_k+2\delta+\Delta)-x(t_k+2\delta)+etc...) \quad (11)$$

$$\langle D_k \rangle = \frac{1}{N} \sum_k D_k \quad (12)$$

is the time average of  $D$  (i.e. the fluence). The noise variance will be defined by

$$\langle D_k^2 \rangle = \frac{1}{N} \sum_k (D_k - \langle D_k \rangle)^2 \quad (13)$$

$$\begin{aligned} \langle D_k^2 \rangle = & \frac{1}{n^2}(2n \langle x^2 \rangle - 2n \langle x(t)x(t+\Delta) \rangle \\ & + 2 \langle x(t+\Delta)x(t+\Delta+\delta) \rangle + 2 \langle x(t+\Delta)x(t+\Delta+2\delta) \rangle + \dots \\ & - 2 \langle x(t+\Delta)x(t+\delta) \rangle - 2 \langle x(t+\Delta)x(t+2\delta) \rangle - 2 \langle x(t+\Delta)x(t+3\delta) \rangle - \dots \\ & - 2 \langle x(t)x(t+\Delta+\delta) \rangle - 2 \langle x(t)x(t+\Delta+2\delta) \rangle - 2 \langle x(t)x(t+\Delta+3\delta) \rangle - \dots \\ & + 2 \langle x(t)x(t+\delta) \rangle + 2 \langle x(t)x(t+2\delta) \rangle + 2 \langle x(t)x(t+3\delta) \rangle + \dots) \\ & (n-1) \text{ similar terms} \\ & + 2 \langle x(t+\Delta+\delta)x(t+\Delta+2\delta) \rangle + 2 \langle x(t+\Delta+\delta)x(t+\Delta+3\delta) \rangle + \dots \\ & - 2 \langle x(t+\Delta+\delta)x(t+2\delta) \rangle - 2 \langle x(t+\Delta+\delta)x(t+3\delta) \rangle \\ & \qquad \qquad \qquad - 2 \langle x(t+\Delta+\delta)x(t+4\delta) \rangle - \dots \\ & - 2 \langle x(t+\delta)x(t+\Delta+2\delta) \rangle - 2 \langle x(t+\delta)x(t+\Delta+3\delta) \rangle \\ & \qquad \qquad \qquad - 2 \langle x(t+\delta)x(t+\Delta+4\delta) \rangle - \dots \\ & + 2 \langle x(t+\delta)x(t+2\delta) \rangle + 2 \langle x(t+\delta)x(t+3\delta) \rangle + 2 \langle x(t+\delta)x(t+4\delta) \rangle + \dots) \\ & (n-2) \text{ similar terms} \\ & (...)\text{The summation is continued in the same way} \end{aligned}$$

The correlated products can be explicitly expressed in terms of the power spectrum as in the previous section



## D The summed results

The summation in equation (14) involves to different series.

$$\begin{aligned}
& \cos(\omega\delta) + \cos(2\omega\delta) + \dots + \cos((n-1)\omega\delta) \\
&= \text{Re}\{e^{i\omega\delta}(1 + e^{i\omega\delta} + e^{2i\omega\delta} + \dots e^{i(n-2)\omega\delta})\} \\
&= \text{Re}\left\{e^{i\omega\delta} \frac{1 - e^{i(n-1)\omega\delta}}{1 - e^{i\omega\delta}}\right\}
\end{aligned} \tag{15}$$

Similarly

$$\begin{aligned}
& \cos(\omega\delta) + 2\cos(2\omega\delta) + \dots + (n-1)\cos((n-1)\omega\delta) \\
&= \frac{1}{\delta} \frac{\partial}{\partial \omega} (\sin(\omega\delta) + \sin(2\omega\delta) + \dots + \sin(n-1)\omega\delta) \\
&= \frac{1}{\delta} \frac{\partial}{\partial \omega} \text{Im}(e^{i\omega\delta}(1 + e^{i\omega\delta} + e^{2i\omega\delta} + \dots e^{i(n-2)\omega\delta}) \\
&= \frac{1}{\delta} \frac{\partial}{\partial \omega} \text{Im}\left\{e^{i\omega\delta} \frac{(1 - e^{i(n-1)\omega\delta})}{1 - e^{i\omega\delta}}\right\}
\end{aligned} \tag{16}$$

The Fowler(n) averages expressions can then be derived

## E Explicit result for the real part

$$\begin{aligned}
(1 - e^{i\omega\delta}) &= 1 - \cos\omega\delta - i\sin\omega\delta = 2\sin^2(\omega\delta/2) - 2i\sin\omega\delta/2\cos\omega\delta/2) \\
(1 - e^{i\omega\delta}) &= -2i\sin(\omega\delta/2)e^{i\omega\delta/2}
\end{aligned}$$

$$\frac{e^{i\omega\delta}}{1 - e^{i\omega\delta}} = \frac{e^{i\omega\delta}}{-2i\sin(\omega\delta/2)e^{i\omega\delta/2}} = \frac{i}{2} \frac{e^{i\omega\delta/2}}{\sin(\omega\delta/2)}$$

The cosine summation is

$$\frac{4}{n} \text{Re}\left(\frac{ie^{i\omega\delta/2}}{\sin(\omega\delta/2)}(1 - e^{i\omega(n-1)\delta/2})\right)$$

As

$$(1 - e^{i\omega(n-1)\delta}) = -2i\sin(\omega(n-1)\delta/2)e^{i\omega(n-1)\delta/2}$$

The real part contribution to the variance  $\langle D_k^2 \rangle$  is

$$\frac{4}{n} \frac{\cos(n\omega\delta/2)\sin((n-1)\omega\delta/2)}{\sin(\omega\delta/2)} (1 - \cos\omega\Delta) \left(A + \frac{B}{\omega^\alpha}\right) \tag{17}$$

## F Explicit results for the imaginary part

$$\begin{aligned}
& -\frac{4}{n^2} \frac{1}{\delta} \frac{\partial}{\partial \omega} \text{Im} \left( e^{i\omega\delta} \frac{(1 - e^{i(n-1)\omega\delta})}{1 - e^{i\omega\delta}} \right) \\
&= -\frac{4}{n^2} \frac{1}{\delta} \frac{\partial}{\partial \omega} \text{Im} \left( \frac{-2i \sin(\omega(n-1)\delta/2) e^{i\omega(n-1)\delta/2} e^{i\omega\delta/2}}{-2i \sin(\omega\delta/2)} \right) \\
&= -\frac{4}{n^2} \frac{1}{\delta} \frac{\partial}{\partial \omega} \frac{\sin(\omega(n-1)\delta/2)}{\sin\omega\delta/2} \text{Im}(e^{i\omega\delta/2})
\end{aligned}$$

This contribution to  $\langle D_k^2 \rangle$  is

$$-\frac{4}{n^2} \frac{1}{\delta} \frac{\partial}{\partial \omega} \frac{\sin(\omega(n-1)\delta/2)}{\sin\omega\delta/2} \sin\omega(n\delta/2) (1 - \cos\omega\Delta) \left( A + \frac{B}{\omega^\alpha} \right)$$

After evaluating the derivative, the imaginary part contribution is

$$\frac{2}{n^2 \sin^2(\omega\delta/2)} (\sin^2(n\omega\delta/2) - n \sin(\omega(2n-1)\delta/2) \sin(\omega\delta/2)) (1 - \cos\omega\Delta) \left( A + \frac{B}{\omega^\alpha} \right) \quad (18)$$

## G The final formula

Adding the real and imaginary contributions obtained in eq. (17) and (18)

$$\begin{aligned}
\langle D_k^2 \rangle &= \int d\omega (1 - \cos\omega\Delta) \left( A + \frac{B}{\omega^\alpha} \right) \left[ \frac{2}{n} \right. \\
&+ \frac{4 \cos(n\omega\delta/2) \sin((n-1)\omega\delta/2)}{n \sin(\omega\delta/2)} \\
&+ \left. \frac{2}{n^2 \sin^2(\omega\delta/2)} (\sin^2(n\omega\delta/2) - n \sin(\omega(2n-1)\delta/2) \sin(\omega\delta/2)) \right] \quad (19)
\end{aligned}$$

**B vs A, 1 and 2  $\sigma$  contours,  $\alpha=0.62$**

